Experimental Operating Plan: Ver 3.2

The Muon $g-2$ Experiment

Fermilab E989

October 1, 2017

David W. Hertzog, Co-Spokesperson

University of Washington

Tel: 206-543-1493

Email: hertzog@uw.edu

Chris Polly, Co-Spokesperson

Fermilab

Tel: 630-840-2552

Email: polly@fnal.gov

Muon $(g-2)$ E989 Collaboration

T. Albahri,[28] S. Al-Kilani,[25] D. Allspach,[7] A. Anastasi,[15,a] A. Anisenkov,[4,b] K. Badgley,[7] S. Baessler,[33,c] I. Bailey,[16,d] V.A. Baranov,[13] E. Barzi,[7] A. Basti,[9] F. Bedeschi,[9] M. Berz,[17] H.P. Binney,[34] R. Bjorkquist,[6] T. Bowcock,[28] G. Cantatore,[11,e] R.M. Carey,[2] J. Carroll,[28] B. Casey,[7] D. Cauz,[24,f] S. Ceravolo,[15] S. P. Chang,[14] A. Chapelain,[6] S. Chappa,[7] S. Charity,[28] R. Chislett,[25] C. Stoughton,[7] T.E. Chupp,[30] M. Convery,[7] A. Conway,[29] G. Corradi,[15] J. Crnkovic,[3] S. Dabagov,[15,g] P.T. Debevec,[26] S. Di Falco,[9] P. Di Meo,[8] G. Di Sciascio,[10] R. Di Stefano,[8,h] B. Drendel,[7] A. Driutti,[24,f] V.N. Duginov,[13] C.J.R. Duncan,[6] M. Eads,[19] A. Epps,[19] O. Escalante-Aguirre,[8,i] O. Escalante-Aguirre,[19] M. Farooq,[30] R. Fatemi,[27] C. Ferrari,[9,j] M. Fertl,[34] A. Fiedler,[19] A.T. Fienberg,[34] A. Fioretti,[9,j] D. Flay,[29] H. Friedsam,[7] E. Frlez,[33] N.S. Froemming,[34] J. Fry,[33] C. Fu,[21,k] C. Gabbanini,[9,j] S. Ganguly,[26] A. Garcia,[34] J. George,[32] L.K. Gibbons,[6] A. Gioiosa,[23,l] K.L. Giovanetti,[12] C.J. Glaser,[33] W. Gohn,[27] T. Gorringe,[27] J. Grange,[1] F. Gray,[20] S. Haciomeroglu,[5] T. Halewood-Leagas,[28] D. Hampai,[15] F. Han,[27] E. Hazen,[2] J. Hempstead,[34] A.T. Herrod,[28,d] D.W. Hertzog,[34] R. Hipple,[17] J.L. Holzbauer,[31] R. Hong,[1] M. Iacovacci,[8,i] M. Incagli,[9] C. Johnstone,[7] J.A. Johnstone,[7] P. Kammel,[34] M. Karuza,[11,m] J. Kaspar,[34] D. Kawall,[29] L. Kelton,[27] A. Keshavarzi,[28] K.S. Khaw,[34] N.V. Khomutov,[13] B. Kiburg,[7] O. Kim,[14] S.C. Kim,[6] Y.I. Kim,[5] B. King,[28] N. Kinnaird,[2] M. Korostelev,[16,d] I. Kourbanis,[7] V.A. Krylov,[13] A. Kuchibhotla,[26] N.A. Kuchinskiy,[13] M. Lancaster,[25] M.J. Lee,[5] S. Lee,[5] B. Li,[21,k] D. Li,[21,n] L. Li,[21,k] I. Logashenko,[4,b] G. Lukicov,[25] A. Lusiani,[9,o] A. L. Lyon,[7] B. MacCoy,[34] K. Makino,[17] S. Marignetti,[8,h] S. Mastroianni,[8] S. Maxfield,[28] W. Merritt,[7] A.A. Mikhailichenko,[6] J.P. Miller,[2] J.P. Morgan,[7] D. Moricciani,[10] W.M. Morse,[3] J. Mott,[2] E. Motuk,[25] A. Nath,[8,i] H. Nguyen,[7] Y. Orlov,[6] R. Osofsky,[34] J.-F. Ostiguy,[7] G. Pauletta,[24,f] G. Pezzullo,[9] G. Piacentino,[23,l] K.T. Pitts,[26] B. Plaster,[27] D. Pocanic,[33] N. Pohlman,[19] C. Polly,[7] J. Price,[28] B. Quinn,[31] N. Raha,[10] E. Ramberg,[7] N.T. Rider,[6] J.L. Ritchie,[32] B.L. Roberts,[2] M. Rominsky,[7,p] D.L. Rubin,[6] L. Santi,[24,f] C. Schlesier,[26] A. Schreckenberger,[32] Y.K. Semertzidis,[5,q] Y.M. Shatunov,[4] D. Sim,[28] M.W. Smith,[9,34] A. Smith,[28] J. Stapleton,[7] D. Still,[7] D. Stöckinger,[22] D. Stratakis,[7] T. Stuttard,[25] H.E. Swanson,[34] D.A. Sweigart,[6] M.J. Syphers,[19] D. Tarazona,[17] T. Teubner,[28] A.E. Tewlsey-Booth,[30] K. Thomson,[28] V. Tishchenko,[3] N.H. Tran,[2] W. Turner,[28] E. Valetov,[17] G. Venanzoni,[9] V.P. Volnykh,[13] T. Walton,[7] Y. Wang,[2] M. Warren,[25] L. Welty-Rieger,[7] M. Whitley,[28] P. Winter,[1] A. Wolski,[28,d] E. Won,[5] M. Wormald,[28] W. Wu,[31] H. Yang,[21,k] and C. Yoshikawa[7]

[1]*Argonne National Laboratory*

[2]*Boston University*

[3]*Brookhaven National Laboratory*

[4]*Budker Institute of Nuclear Physics*

[5]*Center for Axion and Precision Physics (CAPP) / Institute for Basic Science (IBS)*

[6]*Cornell University*

[7]*Fermi National Accelerator Laboratory*

[8]*INFN, Sezione di Napoli*

[9]*INFN, Sezione di Pisa*

[10]*INFN, Sezione di Roma Tor Vergata*

[11]*INFN, Sezione di Trieste*

[12]*James Madison University*

[13]*Joint Institute for Nuclear Research*

[14]*Korea Advanced Institute of Science and Technology (KAIST)*

[15]*Laboratori Nazionali di Frascati*

[16]*Lancaster University*

[17]*Michigan State University*

[18]*North Central College*

[19]*Northern Illinois University*

[20]*Regis University*

[21]*Shanghai Jiao Tong University*

[22]*Technische Universität Dresden*

[23]*Universitá di Molise*

[24]*Universitá di Udine*

[25]*University College London*

[26]*University of Illinois at Urbana-Champaign*

[27]*University of Kentucky*

[28]*University of Liverpool*

[29]*University of Massachusetts*

[30]*University of Michigan*

[31]*University of Mississippi*

[32]*University of Texas at Austin*

[33]*University of Virginia*

[34]*University of Washington*

(Dated: Sunday 1st October, 2017)

PACS numbers:

DISCLAIMER

[a]Also at Universitá di Messina
[b]Also at Novosibirsk State University
[c]Also at Oak Ridge National Lab
[d]Also at The Cockcroft Institute
[e]Also at Universitá di Trieste
[f]Also at INFN, Sezione di Trieste
[g]Also at Lebedev Physical Institute and NRNU MEPhI
[h]Also at Universitá di Cassino
[i]Also at Universitá di Napoli
[j]Also at Istituto Nazionale di Ottica - Consiglio Nazionale delle Ricerche
[k]Also at Shanghai Key Laboratory for Particle Physics and Cosmology
[l]Also at INFN, Sezione di Lecce
[m]Also at University of Rijeka
[n]Also at China University of Geosciences (Wuhan)
[o]Also at Scuola Normale Superiore di Pisa
[p]Also at North Central College
[q]Also at Korea Advanced Institute of Science and Technology (KAIST)

Contents

I. INTRODUCTION

The Muon $g-2$ Experiment E989 at Fermilab will measure the muon's anomalous magnetic moment, $a_\mu \equiv (g-2)/2$, to unprecedented precision: the goal is 0.14 parts per million (ppm). The worth of such an undertaking is coupled to the fact that the Standard Model (SM) prediction for a_μ can also be determined to similar precision. As such, the comparison between experiment and theory provides one of the most sensitive tests of the completeness of the model.

The Brookhaven-based E821 experiment completed data taking in 2001. Their final result determined a_μ(Expt) to 0.54 ppm. Steady improvements in theory since that time have resulted in a present SM uncertainty on a_μ(SM) of 0.42 ppm, and many new efforts are promising to reduce the uncertainty much further. At present, the experimental measurement and SM predictions differ more than 3.6 standard deviations.

The experimental design is anchored by the re-use of the existing precision muon storage ring, an efficient and parasitic deployment of the Fermilab proton complex and beamlines, and strategic upgrades or replacements of outdated or under-performing components from E821. At the time of this EOP, the storage ring magnet has been operated in the new MC-1 building for more than a year, and its precision field has been shimmed to a uniformity exceeding that achieved at BNL by a factor of ~ 3. The storage ring subsystems – inflector, (new) kicker, quads, collimators –

have all been installed and tested, but some improvements are required for them to meet design performance. The calorimeters, auxiliary detectors, fast data acquisition, and full calibration systems have been installed either completely, or nearly completely and have been tested since spring, 2017. The entire experiment was tested in parallel with the beam commissioning period in spring, 2017. The experiment received test "shots" of injected beam at various times during a six-week period. The Delivery Ring was not yet commissioned, so a combined proton/pion/muon beam was directed to the $g-2$ ring. A report on the commissioning lessons learned will be provided at the Operational Readiness Review. An executive summary is that all systems essentially worked — no major failures — but so far the muon storage rate is quite low and we are working in many areas to improve it to meet design expectations.

II. SCIENCE

Muon $g-2$ is a special quantity because it can be both measured and predicted to sub-ppm precision, enabling the $g-2$ test for new physics defined by $a_\mu^{\rm New} \equiv a_\mu^{\rm Exp} - a_\mu^{\rm SM}$. As a flavor- and CP-conserving, chirality-flipping, and loop-induced quantity, a_μ is especially sensitive to new physics contributions [1].

The 2016 updated $g-2$ comparison to theory [2] gives:

$$\Delta a_\mu^{\rm New} = [(274) \pm 76] \times 10^{-11} \quad (3.6)\,\sigma. \tag{1}$$

The goal of Fermilab E989 is to reduce the experimental uncertainty of a_μ by a factor of 4; that is, $\delta a_\mu \sim 16 \times 10^{-11}$, a relative uncertainty of 140 ppb. In the 12 years that have passed since the BNL result [3], the Standard Model (SM) uncertainty has been reduced by a factor of 2. Anticipated theory improvements on the timescale of E989 data taking aim to reach the uncertainty goal of the experiment; see Fig. 1

A. The Standard Model Inputs

The SM terms are usually listed in five categories:

$$a_\mu^{\rm SM} = a_\mu^{\rm QED} + a_\mu^{\rm Weak} + a_\mu^{\rm HVP} + a_\mu^{\rm Had-HO} + a_\mu^{\rm HLbL}. \tag{2}$$

The QED, Weak, and hadronic higher-order (Had-HO) terms have negligible uncertainties. The hadronic vacuum polarization (HVP) contribution [2] is determined from experiment through a dispersion relation that amounts to an energy-weighted integral of $e^+e^- \to \textit{hadron}$ total cross

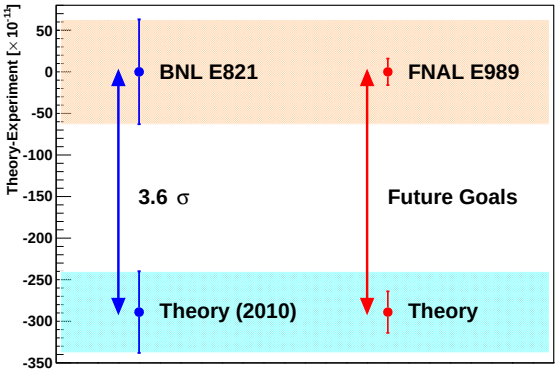

Figure 1: Simple graphic to compare Experiment to Theory at present and, what might be expected on completion of Fermilab E989 and by a twofold reduction in the theory uncertainty.

sections. The uncertainty has been reduced by 21% since the 2011 updates, owing mostly to new data from KLOE, BES, and multi-hadron processes measured at BaBar. It has been evaluated in 2016 with an uncertainty of 33×10^{-11}. The hadronic light-by-light (HLbL) effect is evaluated using models. The quoted uncertainty of 26×10^{-11} is a consensus value reached by comparing models; it is not a well-defined uncertainty. Recent efforts using lattice QCD have made rapid progress toward a complete calculation of HLbL with realistic inputs (quark masses, appropriate lattice sizes). A nearly complete calculation that includes all connected and leading disconnected diagrams has recently been reported by Blum et al. [4]. The authors obtain a statistical uncertainty of 13.5×10^{-11}, a remarkable accomplishment. Systematic studies are required before their central value and final uncertainty can be included in the overall SM evaluation.

B. The Experimental Inputs

The measurement of a_μ is based on the following principles. When a muon with charge q is circulating in the horizontal plane of a magnetic storage ring, its cyclotron revolution frequency is $\vec{\omega}_c = -q\vec{B}/m\gamma$. The muon spin precesses at frequency $\vec{\omega}_s = -(gq\vec{B}/2m) - [(1-\gamma)q\vec{B}/\gamma m]$, owing to the torque on the magnetic moment and including the Thomas precession effect for the rotating reference frame [5]. The magnitude of ω_s is greater than ω_c for $g \neq 2$. For perfect fields and no betatron oscillations, the difference is the anomalous precession frequency defined by

$$\vec{\omega}_a \equiv \vec{\omega}_s - \vec{\omega}_c = -\left(\frac{g-2}{2}\right)\frac{q\vec{B}}{m} = -a_\mu \frac{q\vec{B}}{m}, \tag{3}$$

where we have assumed for now a negligible effect from a non-zero electric dipole moment.

Parity violation in $\mu^+ \to e^+ \bar{\nu}_\mu \nu_e$ associates the decay positron energies in the laboratory frame with the average spin direction of the muon at the time of the decay, such that the highest-energy positrons are preferentially emitted when the muon spin is aligned with its momentum and lower-energy positrons are emitted when the spin is reversed. Systems of detectors measure the decay positron times and energies.

To achieve the conditions described above, polarized muon bunches must be injected into the magnet, kicked onto a stable storage orbit, and then observed non-intrusively until they decay. The motional magnetic field seen by a relativistic muon passing through an electric field $\vec{E}$ contributes an important term to the spin precession rate, represented by

$$\vec{\omega}_a = -\frac{q}{m}\left[a_\mu \vec{B} - \left(a_\mu - \frac{1}{\gamma^2 - 1}\right)\frac{\vec{\beta} \times \vec{E}}{c}\right]. \tag{4}$$

At $p_\mu = 3.094$ GeV/c, ($\gamma = 29.4$), the 2nd term in Eq. 4 exactly vanishes. The residual effect for muons slightly off the magic momentum, and therefore not centered in the null region of the electric quadrupoles, results in an E-field correction to the measured precession frequency. The beam also executes horizontal and vertical betatron motions at frequencies determined by the weak-focussing index of the storage ring (i.e, the electric field strength). The vertical undulation of the muons means $\vec{p}_\mu$ is not exactly perpendicular to $\vec{B}$, thus a small "pitch" correction is necessary. Combined, these corrections shift a_μ by $86(6) \times 10^{-11}$ [6]; the error was negligible in E821, but will need to be reduced for E989. This will be accomplished by more sophisticated particle tracking and by indirect measurements of the muon beam profile vs. time, obtained by using our new in-vacuum Straw Tracker system.

The quantity $a_\mu^{\rm Exp}$ is obtained from the independent measurements of the anomalous precession frequency and the average integrated magnetic field. Calorimeters are used to measure the anomalous precession frequency ω_a and pulsed proton NMR to measure the magnetic field in terms of the proton Larmor precession frequency, ω_p. Both measurements involve frequencies that are referenced to highly stable precision oscillators. It is further necessary to know the muon distribution in the storage ring for the muon population that contributes to the ω_a data. This distribution is folded with similarly determined azimuthally averaged magnetic field moments to give the effective magnetic field seen by the muons, $\tilde{\omega}_p$ below. Given these experimentally determined quantities, one obtains a_μ at the precision needed through the relation

$$a_\mu^{\rm Exp} = \frac{g_e}{2}\frac{\omega_a}{\tilde{\omega}_p}\frac{m_\mu}{m_e}\frac{\mu_p}{\mu_e}. \tag{5}$$

In this expression, our $g-2$ experiment will report the ratio of the muon precession frequency to the proton precession frequency, $R \equiv \omega_a/\tilde{\omega}_p$, where all systematic errors from the separate

Table I: Uncertainties on the quantities used to determine $a_\mu^{\rm Exp}$ and $a_\mu^{\rm SM}$. Experimental errors from Ref [6]. CODATA ratio uncertainties from the 2014 online update.

Quantity	Present Uncertainty	E989 Goal
	ppb	ppb
Total ω_a Statistical	460	100
Final ω_a Systematic	210	70
Final $\tilde{\omega}_p$ Systematic	170	70
CODATA m_μ/m_e	22	–
CODATA μ_p/μ_e	3.0	NA
Electron g factor, g_e	0.000035	NA
Final E821	630	–
Goal Fermilab E989	–	140

uncertainty table entries are appropriately evaluated and combined in the uncertainty on R. From external experiments, one obtains the electron g_e factor [7], the muon-to-electron mass ratio, and the proton-to-electron magnetic moment ratio, [8]. These quantities are all known quite well. Table I summarizes the latest versions of the absolute and relative uncertainties of the theoretical and experimental quantities.

III. OVERVIEW OF THE EXPERIMENTAL TECHNIQUE

A. The experiment in a series of steps

1. For each 1.4 s accelerator cycle—see Fig.2—four Booster batches of 8 GeV protons are injected into the Recycler; there they are divided into four proton bunches.

2. Each $\sim 10^{12}$ proton bunch is directed one at a time to the $g-2$ Target Station located in the AP0 hall. The magnets direct 3.1 GeV/c positive secondaries into the M2 beamline.

3. Forward-decay, highly polarized muons from $\pi^+ \to \mu^+\nu_\mu$ decay, are captured in the FODO lattice of the M2/M3 beamline.

4. The π, μ and p secondaries are directed into the Delivery Ring (DR). After four circulations, no pions remain. Protons—which travel slower than muons—are removed by a kicker.

5. After the fourth turn in the DR, a pure $\sim$ 95% polarized muon bunch is extracted into the M4/M5 beamline and directed through the superconducting inflector corridor into the storage ring (SR).

Table II: Various parameters for the Fermilab E989 Experiment.

Parameter	Fermilab E989
Magnetic field	1.45 T
Radius	711 cm
Revolution period	149.1 ns
Precession frequency, ω_a	1.43 MHz
Lifetime, $\gamma\tau_\mu$	64.4 μs
Typical asymmetry, A	0.4
Beam polarization	> 0.95
Events in final fit	1.5×10^{11}

6. A fast kicker deflects the muons onto stable orbits within the storage volume. Electric quadrupoles provide weak focussing to contain the beam.

7. Auxiliary scintillating fiber and straw tracker detector systems are used to help guide the beam injection process and to determine key beam dynamic storage properties.

8. As muons circulate the SR, their spins precess at a rate proportional to $g-2$ and to the strength of the magnetic field. Determination of the precession frequency ω_a is made through the correlation of the measured decay positron energy spectrum—measured by calorimeters—to the spin direction of the muon at the time of decay.

9. The relative and absolute magnetic field is determined by pulsed NMR methods. Fixed probes above and below the vacuum chambers continuously monitor the field during data taking, while mapping of the field in the actual storage volume is made periodically using an in-vacuum NMR trolley.

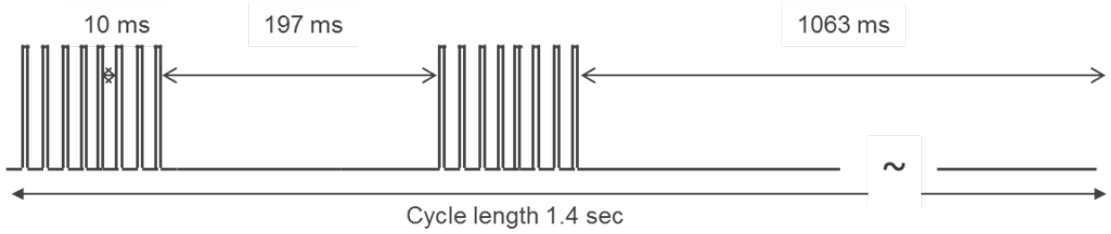

Figure 2: The current Laboratory default 21 Booster tick cycle in a 1.4 s cycle. The 16 bunches available to $g-2$ are derived from four Booster batches.

B. Major experimental equipment and instrumentation

1. **The (E821) Storage Ring (SR):** The 1.45 T magnetic field is produced by three superconducting coils connected in series. The current is maintained to a few ppm precision based on a feedback loop incorporating a subset of the pNMR probes to the main power supply (see below). Final course shimming has resulted in field uniformity exceeding that obtained at BNL by a factor of 3 or better.

2. **The Inflector:** The superconducting double cosine magnet that largely cancels the SR field along the injection corridor. The E821 inflector, with its closed ends, will be used initially. A design for an open-ended inflector has been largely completed. If realized, the throughput of muons in the SR will increase by $\approx 50\%$.

3. **The SR Kicker:** This new device produces a transverse outward magnetic kick to the incoming muon bunch during the first turn, which deflects the muons onto a stable orbit. In practice, three independent kickers energize three sets of plates located about a quarter way around the ring following injection. Tuning the Kicker timing and voltages will be a major part of initial commissioning to optimized muon storage.

4. **The Electrostatic Quadrupoles:** Four regions of the storage ring contain plates that produce a static quadrupole electric field. They provide weak focussing for the muons. The quads are initially asymmetrically energized to scrape the muons onto beam-storage-defining collimators. When relaxed to a symmetric configuration, the muon beam should be well contained inside the 9-cm-diameter volume. The quads are powered by four PS cabinets located near the center of the SR. Typical operating voltage in the range $21 - 32\,\mathrm{kV}$.

5. **Vacuum Chamber System:** 12 scalloped vacuum chambers housing the rail system to guide the pNMR Trolley, the quadrupole plates, the kicker plates, and the collimator system, the latter of which resides in the flexible bellow sections between discrete VC sections.

6. **Calorimeter Stations:** 24 stations are located symmetrically around the inside of the SR. Each self-contained station includes a 54-element PbF_2 crystal calorimeter with SiPM readout and an optical front panel for calibration. The mechanical housing chariot contains a Beaglebone controlled bias voltage system, a MicroTCA housed bank of 800 MSPS 12-bit digitizers, a low-voltage distribution system, ethernet distribution, a calorimeter cooling system, power distribution, and safety interlocks.

7. **Calibration System:** A Laser Hut located under the MC-1 loading dock houses an optics distribution containing six fast laser heads, splitters to allow for source and local monitoring of the pulses, filter wheels to provide calibration protocols, and local electronics to measure both outgoing and returning light levels from the calorimeter stations. 24 fiber conduits allow for optical fiber distribution to deliver and receive light from the calorimeters.

8. **Straw Tracker System:** A Tracker consists of eight identical modules, each containing 128 straw drift tubes, arranged in four planes oriented in a UV configuration. The Tracker active region is located in vacuum, in the scallop region immediately upstream of a calorimeter station. The onboard digitizing electronics convey hit times to a microTCA housed TDC system. Two Trackers will be installed for the FY18 running period.

9. **Auxiliary Detectors:** A T0 scintillator immediately outside of the SR provides a time and intensity profile of the incoming muon bunch. Two scintillating fiber hodoscopes at the inflector corridor entrance and intermediate location each provide an XY-profile of the incoming beam. Fiber Harp detectors provide X and Y profiles of the stored muon beam at two locations inside the SR volume. These destructive devices are used to map the stored muon profile; they are retracted during normal data collection.

10. **Absolute Field Measurement System:** The magnetic field measurement is based on a series of pNMR measurements using different devices, each with particular features. A particularly spherical "absolute" NMR probe will determine the field magnitude for $g-2$ and tie it to the experiments measuring muonium hyperfine transitions. A moveable "plunging" probe is located in an especially uniform region of the SR magnetic field. It can be maneuvered to determine the field in the XY locations corresponding to the NMR Trolley probes (see next).

11. **Field Mapping Trolley:** An in-situ non-magnetic trolley carries an array of 17 pNMR probes on its front face. It is pulled through the SR volume to provide a complete field map in the volume where the muons circulate. This procedure will be done either daily or every few days.

12. **Fixed Probes System:** A set of 378 pNMR probes are permanently mounted to grooves on the top and bottom plates of the vacuum chambers. They are read out continuously to provide a measure of the magnetic field stability vs. time. A subset is used to control the SR power supply.

C. Operational Sequence to Arrive at Physics-Quality Data Taking

We describe next four relatively distinct tasks and optimizations that each must achieve success to meet the goals of E989.

1. Muon beam to the Storage Ring

Muon $g-2$ expects a beam of almost pure muons to arrive at the Storage Ring (SR) entrance with an intensity of $\approx 8 \times 10^5$ in a $\Delta P/P = 2\%$ momentum bite. AD will optimize the RF re-bunching of proton batches in the Recycler to from 4 bunches per batch, each with a temporal width of no more than 120 ns. These bunches are directed onto the pion target with a focus small enough to generate pions in excess of 10^8/bunch that are captured in the M2 FODO lattice in a $\Delta P/P = 0.5\%$ momentum bite. Transporting this beam — which is decaying into forward spin muons — through M3, into the Delivery Ring (DR), around it n times (a variable), and extracting to the M4 and then M5 lines, is expected to be done with 90% efficiency. The beam Twiss parameter at the SR entrance, including the (x,x') and (y,y') profiles, can be adjusted by tuning optimization. The goal is to produce a beam which can squeeze through the narrow inflector full aperture (18×56 mm^2. The Collaboration supplies instrumentation (T0 and IBMS 1 and 2) to measure the timing, the intensity and the XY profiles following the last beam element wire chamber and terminating inside the SR magnet at the inflector entrance. It is expected that optimizing this beam will take several months in FY18.

AD is fully responsible to bring the beam to the SR. Several AD members are key E989 collaborators. Non-AD collaborators have done three independent end-to-end beamline simulations of this sequence and they are expected to work with AD beam tuners to perfect the beam. E989 detector experts have prepared the entrance counters and will analyze the data and provide fast feedback.

2. Muon storage

The muon storage fraction from a beam prepared as above is expected to be approximately $2 \pm 0.5\%$ with respect to the incoming flux. This is mainly determined by the small momentum acceptance of the SR, $\Delta P/P \approx 0.15\%$. The storage fraction can be significantly lower if the ring elements are not optimized. This requires a disciplined approach to tuning the inflector current, the quadrupole voltages (tune), the three SR kicker timings, and the three kicker field strengths. Two

sets of in-vacuum scintillating "Fiber Harp" hodoscopes are used to monitor the stored beam. They provide turn-by-turn imaging of the beam profile, which is analyzed to yield the Mean and Width vs. time for both horizontal and vertical projections. This information also encodes the coherent betatron oscillation (CBO) frequency and amplitudes. Centering the beam and minimizing the CBO amplitudes is a requirement for optimized beam storage. While the horizontal centering is affected by the kicker, the vertical is quite sensitive to the average residual radial magnetic field in the storage ring. The radial field can be adjusted everywhere in azimuth using the surface coil system. Accurate determination of the vertical beam mean is provided by the segmented calorimeters. This was tested in the commission run and worked as predicted.

A fill-by-fill, online metric of beam storage intensity is provided using an algorithm of high-energy pulse counting from the 24 calorimeter stations, the CTAG signal. Tracking CTAGs vs. tuning optimization is rapid; once optimized, accumulating data for a short period of time then allows a detailed Fiber Harp image to be built. These tools exist in online and offline, respectively. The detectors and their corresponding analyses were successfully used in the 2017 commissioning run and have become routine tools. The key to increasing muon storage is a patient, iterative approach to sweeping over the tuning knobs for each setting of the incoming beam (section above). The E989 collaboration uses three simulation tools to guide this work; each is maintainedcross by different collaborating groups.

The overall muon storage topic is led by a Beam Dynamics group that meets weekly. A cross-collaboration Task Force was established following the commissioning run to investigate all factors that effected the then realized muon storage fraction. They have prepared a preliminary report of missing factors from initial proton flux, to storage non-optimization. Their observations are being addressed during the shutdown.

3. Precession frequency and beam quality measurement

The precession frequency, ω_a, measurement is mainly accomplished by the calorimeter system, which includes 1296 individual crystals, each readout continuously by a 800 MSPS, 12-bit-depth digitizer. To be effective, each crystal must first be gain matched to approximately 10%. This is accomplished by the laser system that distributes short bursts of photons to each crystal with a highly stable shot-to-shot output stability. Such data is used to make an absolute calibration in pe/mV output for each crystal. Variable gain amplifiers are then used to tune gains to approximately match. This system has been used for more than a year, starting with SLAC test beams,

and through the commissioning run of 2017.

During data taking fills, any pulse above a nominal low threshold in any of the 54 crystals of a calorimeter station triggers saving the waveforms for all crystals within a present time window of the pulse. Thus, the data is accumulated in hardware in a lossless manner and saved using a zero-suppressed lossless procedure. A GPU farm is responsible for this data selection online. Approximately 100 MB/s are saved.

To maintain gain stability at $\approx 10^{-4}$ level during a fill, and $\approx 10^{-3}$ longer term, the laser system is fired before and after all fills and, in special runs, during the fills. This builds a data base for gain stability over time. The benchmark stability has been established in a test beam run, but not yet in commissioning owing to the 0.1 Hz fill rate from AD.

The precision Clock and Control system (CCS) is a highly sophisticated distribution of disciplined oscillators that route to each digitizer, (and separately to the NMR system below). The CCS also performs all triggering functions, representing the switchyard for the experiment. The absolute clock frequency will be blinded when data taking begins. A blinded frequency monitoring system is being built that will guarantee clock frequency stability between weekly scheduled inspections by the selected non-E989 collaborator who will set the blinding and maintain the frequency log.

The in-vacuum Tracker detectors record decay positron tracks in two large regions of the SR. Unlike the Fiber Harps, which are destructive and must be retracted during physics data taking, the Trackers are passive and record all decays within their fiducial volume. The information is analyzed to trace the decay track back to a point of tangency within the SR volume in order to build the profile of the muon distribution that is needed to convolute with the magnetic field (next section) to obtain ω_p. The Trackers will also be used to provide a new limit on the muon's EDM, thus providing an additional physics result.

4. Magnetic field measurement and monitoring

The determination of a_μ from the precession frequency data is incomplete without an equally precise measurement of the average magnetic field seen by the muons whose decays are recorded by the calorimeters. The field measurement, ω_p, includes not only the magnetic field, but also the muon profile (previous section).

The magnetic field measurement is carried out using pulsed proton NMR (pNMR) with a series of water amd petroleum jelly probes. The absolute field is measured using a special highly spherical water probe; it is also the same probe used in the muonium hyperfine experiment that determines

the muon-to-proton magnetic moment ratio. It is cross calibrated with a Plunging Probe (PP) which is located in one area of the SR vacuum, where an extra effort has been made to prepare a highly uniform field region. The in-vacuum NMR Trolley is calibrated in this region against the PP whose moveable arm allows positioning of the PP to each location corresponding to the coordinates of the individual 17 Trolley probes, when the Trolly occupies the same azimuthal region of the PP. Finally, the continuous monitoring of the SR field stability is carried out by 378 Fixed Probes (FP) located above and below the vacuum chambers and distributed uniformly around the ring. A set of FPs are used in a feedback loop to the main SR power supply to keep the field stable over time.

In practice, different groups in the collaboration specialize on the construction, operation, and maintenance of this equipment, and the custom field DAQ. Operationally, the Field Team has been running for over a year as they have completed shimming steps to prepare a highly uniform magnetic field.

During a physics data-taking campaign, one can expect to have first optimized the shimming and mutipole reduction of the azimuthally averaged magnetic field using the Trolley to obtain data, and the hardware shimming knobs, and surface coil currents, to tune the field. A Plunging Probe to Trolley Probe inter calibration exercise will occur no more than monthly. A Trolley mapping of the entire magnetic field (3 - 4 h) will occur every 1 to 3 days, with the frequency tuned once the map to map field stability is better understood in operational mode. We note that during any accelerator down time, we will use the opportunity to carry out a Trolley run if at all possible. The Fixed Probes are always read out; they provide the moment by moment heartbeat for the field stability.

IV. OVERVIEW OF COMPUTING

The computing section of Muon g-2 experiment can be divided mainly into two parts: *online computing* and *offline computing*. *Online computing* includes DAQ, online monitoring, and nearline operation while *offline computing* involves MC simulation, truth digitization, data reconstruction and data analysis.

The main requirements for the *online computing* are the following:

- Accommodate 12 Hz average rate of muon fills that consist of sequences of eight successive 700 μs fills with 10 ms fill-to-fill separations

- Handle 20 GB/s of raw data and reduce it by a factor of 100 for data storage (implemented

using GPU technology)

- Total recorded raw data on tape after 2 years of running will be 6 PB (3 PB for FY 18)

The main requirements for the *offline computing* are the following:

- Generate MC dataset required by the analysis groups in a timely fashion
- Process raw data in a timely fashion after data taking and automate keep-up processing (offline production)
- Total recorded raw data on tape after 2 years of running will be 4 PB (2 PB for FY 18)
- Reproducibility of the data analysis (periodic software release)

A. DAQ and Online Monitoring

At the moment of writing, the DAQ for ω_a and ω_p measurements are independent of each other. Efforts are ongoing at the offline level (e.g. using the common distributed GPS timing signal) to correlate their recorded information.

Precession Frequency Measurement

For the ω_a measurement, information from multiple detectors are aggregated on the fill-by-fill basis at 12 Hz average DAQ rate. Data types from each detector system are briefly described below:

- Photodetector (SiPM) signals from 24 Calorimeters (each has 54 channels) are digitized continuously at 800 MHz for 700 s after receiving an accelerator trigger. Positron or muon pulses that are over the threshold will trigger the GPU farm and will be recorded to disk.
- The tracker station (consisted of 8 tracking modules) will take data for 800 μs after receiving an accelerator trigger and the information will be stored as raw straw hits.
- Scintillating signals from the time zero (T0) counter which are essential for determining the arrival time of the beam are digitized continuously at 800 MHz for several μs.

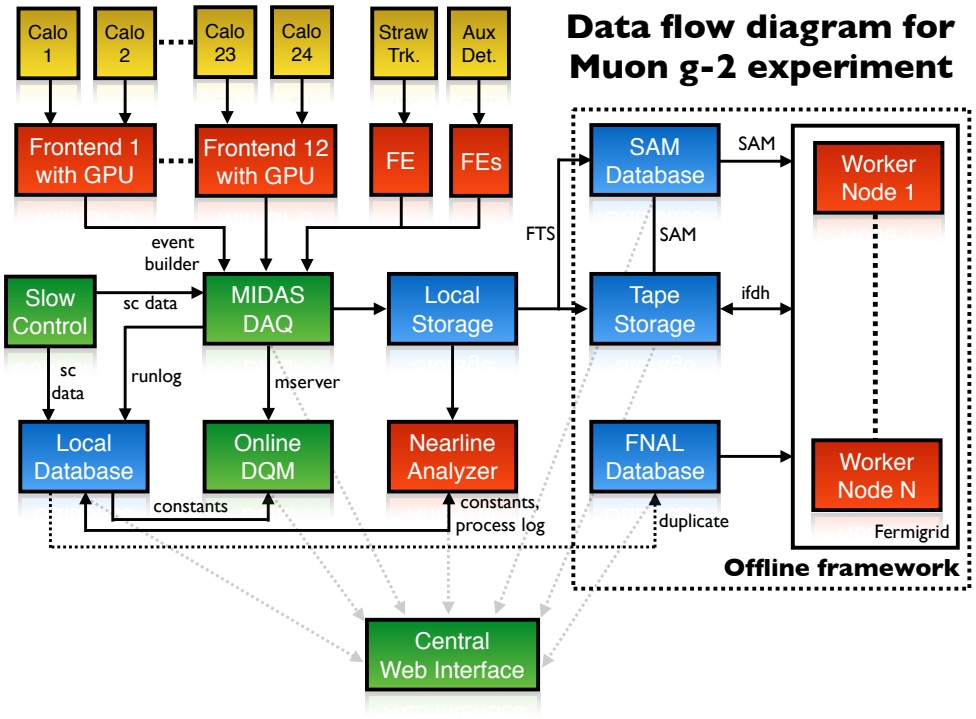

Figure 3: Data flow for ω_a data processing. Similar flow is adopted by the ω_p analysis team.

- Signals from the Electrostatic Quadrupoles (ESQ) and the Pulsed Magnetic Kickers are also digitized (at different rates and lengths) for systematic studies related to the beam timing. Together with T0 and the IBMS, they are collectively called *auxiliary detectors*.

The Muon g-2 data flow is defined as a series of steps of the following:

1. As shown in Fig. 3, these data are then built by the MIDAS DAQ into an event and all the events under the same experimental conditions will form a run.

2. For a smoother data handling, each run is divided into multiple sub-runs where each subrun has simply a file size limit of 2 GB.

3. These files are in a binary format with MIDAS event structure and are written immediately into a local 40 TB RAID6.

4. Then, the completed files are transferred to the dCache area using Fermilabs File Transfer Service (FTS).

5. Offline data unpacking (from binary format to data products) and data reconstruction which are implemented within the art framework then follows using standard FIFE tools.

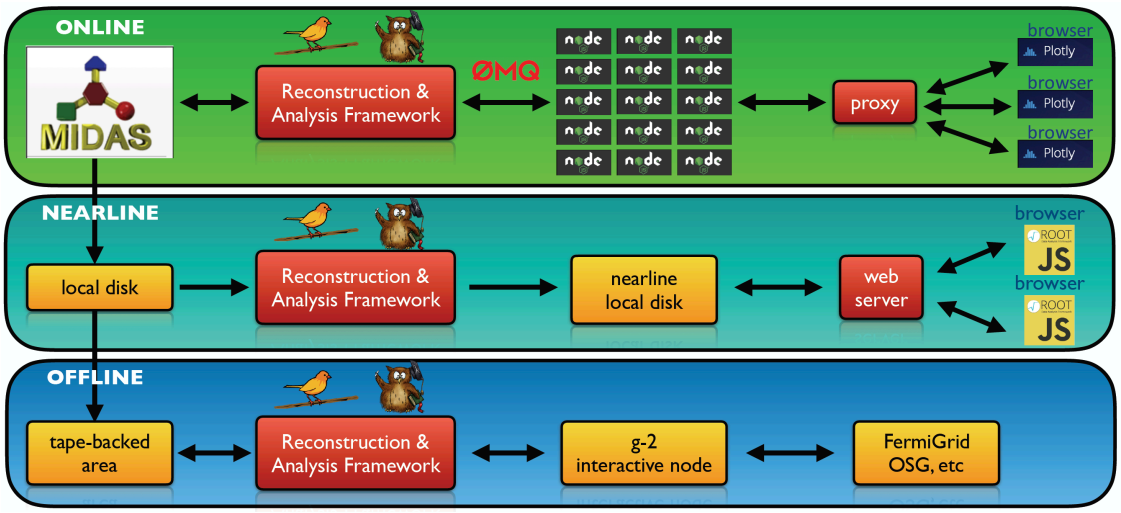

Figure 4: The interplay between online, nearline and offline mode of running the reconstruction and analysis framework.

6. Currently production scripts enable an analyzer to submit a job to the either the FermiGrid or the Open Science Grid (OSG).

The offline reconstruction and analysis codes are also operating in the online and nearline fashion to monitor the live data stream and the recorded raw data. A detailed data flow is depicted in Fig. 4.

- For the online Data Quality Monitor (DQM), reconstructed data is aggregated using Node.js servers.
- These servers then stream the data on demand to users browser running data plotting services like Plotly.
- For the nearline operation, the analyzed data is stored at the highest level in a nearline local disk.
- A web server running JavaScript ROOT (JSROOT) provides almost-live (2-3 minutes after subrun) high-level physics information to users.

Magnetic Field Measurement

The determination of ω_p utilises several distinct measurements of the magnetic field taken at regular intervals which are convoluted with the muon beam distribution. Data is accumulated from four systems:

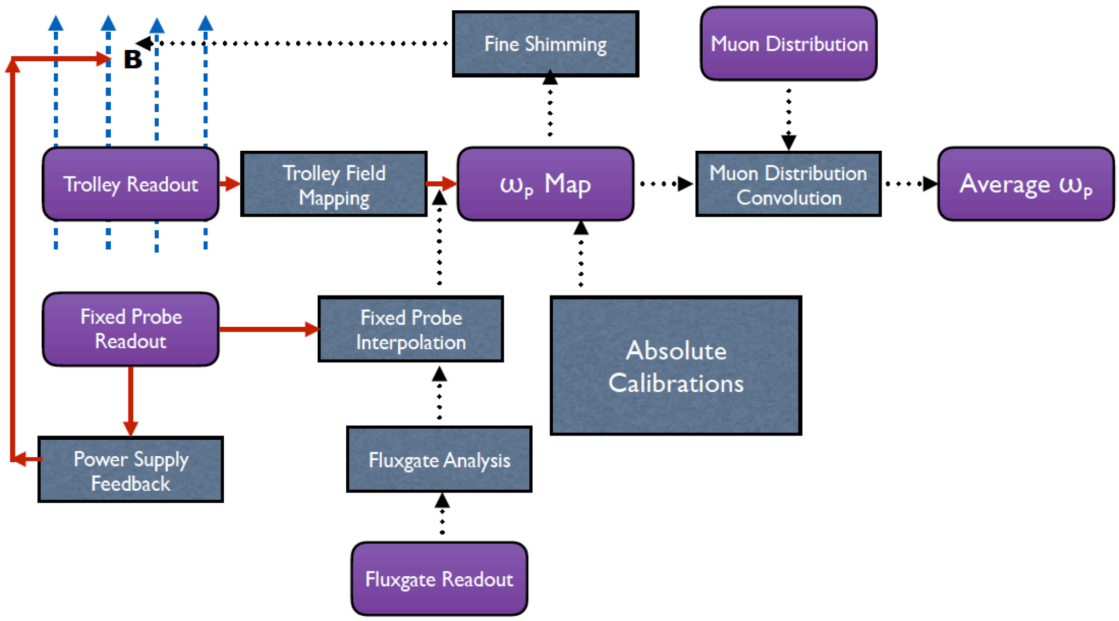

Figure 5: A schematic of the various readout systems used to determine ω_p

- The trolley-probe which moves along rails inside the vacuum chambers and measures the field in the storage region when there is no beam and passes both position data (determined from barcodes on the vacuum chambers) and data from 17 NMR probes on the trolley itself.
- The fixed-probes: 378 of these are somewhat offset from the storage region and will pass NMR data while there is beam.
- The fluxgate magnetometers: 8 of which will measure transient fields close to the storage ring magnet.
- The plunging probe: a water-based probe that is used to calibrate the petroleum-jelly based trolley probe.
- Additionally periodic data will also be accumulated from the surface coils, feedback power supplies and the collimator system.
- A final overall calibration of the plunging probe will be made with independently calibrated water and 3He magnetometers.

A final overall calibration of the plunging probe will be made with independently calibrated water and 3He magnetometers. A schematic of the various readout systems used to determine ω_p is shown in Fig. 5.

The NMR-probes send analog signals to digitizers which create the data that is ultimately processed. The readout of the fixed-probes is fast enough that a data sample can be produced for all 378 probes every 1.4 s accelerator super-cycle. The trolley-probe takes 2 hours to accumulate data at 6,000 locations around the ring and will take data periodically when there is no beam: this would typically be once or twice a day.

The data is accumulated within the experiment-wide MIDAS DAQ system but is asynchronous with respect to the data accumulated by the detector systems for the ω_a determination. The ω_p and ω_a datasets are cross-correlated in time by means of a common, distributed GPS timing signal. The dataset size is dominated by the data from the fixed probes which can in principle record data for every muon spill. Each of the 378 probes produces 100 kB of digitized data per accumulation (5 ms). If data were recorded for every accelerator supercycle (0.75 Hz) then approximately 1 PB of data would be recorded. While there will be times when data is recorded with this frequency, we expect instead to record at approximately 0.02 Hz which along with periodic accumulations of data at a higher frequency is expected to produce a dataset of approximately 25 TB over a two year running period. This is small in comparison with the ω_a dataset. It will be stored on both a RAID-5 array (gm2field-server) and tape.

B. Offline Computing and Data Analysis Plans

Precession Frequency Analysis

Precession Frequency Analysis can be separated into two stages: *reconstruction* and *analysis*. *Reconstruction stage* is a sequence of algorithms transforming recorded islands to proxies for positrons and muons in the following steps:

- **Pulse fitting:** An island is fitted using template waveform
- **Gain calibration:** The fitted hit is gain calibrated using laser calibration technique
- **Energy calibration:** The gain calibrated hit is energy calibrated using MIP signal and endpoint energy calibration techniques
- **Hit Clustering:** The energy calibrated hits are clustered to form a muon or positron candidate

Analysis stage is defined by a series of steps as the following:

- **The modulation of number of high energy positron as a function of time** (in the form of a histogram) is reconstructed from the calorimeter.
- **Positron pileup distribution** is extracted from the calorimeter hit data and correction is applied to the raw histogram above.
- **Distribution of muon losses**, coming from muons leaving the storage ring without decaying, is extracted from the calorimeter data and is included in the fit model of the corrected histogram.
- **Modulations in detector acceptance due to muon beam dynamics** is also included in the fit model.
- **Electric field correction**, due to non-magic-momentum muons, is applied using radial decay distribution extracted from calorimeters and fiber harps de-bunching analyses.
- **Pitch correction**, due to the vertical motion of the muon beam, is applied using vertical decay distribution of the muon extrapolated using tracker stations.

V. DATA PRODUCTION

During the 2017 commissioning run the experiment collected $\approx$ 20 TB of data, which was stored in the form of raw MIDAS banks. Data production proceeds via two steps, unpacking and reconstruction. Unpacking transfers the data in the MIDAS banks into ART data products. Reconstruction then applies a series of algorithms that manipulate the data from raw detector responses into positron signals. This entire process is executed through a single script that is capable of submitting both unpacking and reconstruction jobs, for either data or simulation. The production workflow makes full use of the FIFE tools made available though FNAL Scientific Computing Division (SCD). FTS is used to transfer files to permanent storage, metadata for each production job is stored in the SAM data management system and POMS is utilized to manage job submissions.

Production of the commissioning data utilized both FermiGrid and the OSG. During the commissioning run unpacking kept pace with online data taking, with an average delay of 16 hours. Reconstruction of the entire 20 TB dataset was completed in four days. Table *III* summarizes the format, data size and average memory usage of the data production jobs.

Table III: Commissioning Data Production

Data Tier	Format	Data Size	Memory Usage
raw	MIDAS	20 TB	
unpacked	ART	19 TB	6-8 GB
reconstructed	ART	1.7 TB	4 GB

VI. SIMULATION REQUIREMENTS AND TOOLS

The g-2 collaboration has utilized several simulation packages to design and model the target, injection beamline and storage ring detectors. These same programs are also used to optimize beam injection parameters and provide insight into the systematic effects that may bias the extraction of ω_a. In general, g-2 simulation based studies are grouped into two categories, those concerned primarily with beam optics and those that require full reconstruction of particle Interactions in the storage ring components .

Primary goals of the beam optics studies include a realistic estimate of the final number of muons delivered to the storage ring. This requires modeling of the proton-target interactions and tracking the secondary particles through the beamlines and into the delivery ring. The MARS package was used to simulate proton-target interactions and to model the distribution of downstream secondaries. The G4Beamline (G4BL) simulation package uses this input distribution to track the secondaries through the beamline field apertures and into the storage ring. Although G4BL does include particle interactions such as pion decay and muon spin precession, it does not track particle interactions inside beamline materials. During commissioning both G4BL and BMAD, a comparable optics simulation package, were used to predict the optimal beam injection parameters as well as inflector, kicker and quad fields. Both BMAD and G4BL are used to study the effects of non-optimal quad alignment and field settings on muon storage fractions and muon motion in the ring are ongoing. The COSY simulation package provides the same functionality as BMAD and G4BL, but has the capability to include fringe fields as well. The comparison of G4BL, BMAD and COSY results continue to provide critical cross-checks.

Studies that require full reconstruction of particle interactions in the storage ring components utilize a customized implementation of GEANT within the ART framework called gm2ringsim. The entire ring structure, including passive and active detectors both inside and outside of the storage region, as well as the time-dependent magnetic and electric fields, are implemented in gm2ringsim. This package also includes several types of particle guns that provide the ability to inject a range of particle types and distributions at specific points around the ring. Studies that

utilize the gm2ringsim framework include the development of clustering and track reconstruction in the calorimeter and strawtracker detectors, the development of algorithms to detect the signature of lost muon inside consecutive calorimeters and the study of the muon oscillations around the ring and their effect on beam storage parameters. The gm2ringsim package was also used to study the optimal kicker and quad setting for maximal muon storage and played a critical role in the ultimate design of the new infector magnet.

VII. SIMULATION WORKFLOW

Initial MARS studies were performed at the RACF facility at BNL, but future studies will utilize the MARS implementation at FNAL. Likewise, initial G4BL studies were performed at the NERSC facility at LBL. If availability at NERSC becomes limited it is straightforward to install and run G4BL at FNAL. BMAD is currently installed and running on the FNAL virtual machines. The COSY package is run offsite, currently at Michigan State University. The output of these files is small and does not require a substantial storage footprint.

The production of the gm2ringsim simulation proceeds in two steps and parallels the data production in the second half. The output of the first stage stores the truth level hits in their respective ART data products and takes on average 0.6-6 sec/event depending on the type of gun used and the lifetime of the injected particles. The second stage digitizes the truth level hits for each active detector and consolidates a set number of events into a waveform that represents a single experimental fill. The waveform is then chopped, and fit according to the same procedures implemented in the data. The reconstruction time is an order of magnitude smaller than the truth production. The total output for the gm2ringsim package, truth production and reconstruction combined, is $\approx$ 1TB per 4M events. For the upcoming 2018 run, the collaboration anticipates requiring a gm2ringsim simulation sample that replicates the expected data sample, approximately $1{\times}10^{11}$ events. For the current file sizes this would require a prohibitively large 10 PB of disk space. The collaboration is embarking on a campaign to reduce both the running time and the total storage footprint of the gm2ringsim simulation productions.

Magnetic Field Analysis

The first three stages of data-processing: online, nearline (Tier-0) and the first offline processing (Tier-1) will use *art* and share the same modules. *art* provides a flexible framework to allow

different algorithms to be employed with ease, different dataproducts to be created and has many available utility modules e.g. MIDAStoART. However the nature of the ω_p analysis is somewhat different from the ω_a analysis in that data is accumulated asynchronously from disparate systems, in particular the datasets will often have different run numbers which is the primary key in *art* and cross correlating data across different runs is not straightforward in *art*. For example there will be fixed-probe data accumulated with beam that must be correlated with trolley data accumulated without beam. The *art*/ROOT files from the Tier-1 offline processing will thus then be processed to create bespoke (non-*art*) ROOT files with a well-defined structure better suited to facilitate data correlation between the different systems.

A common toolkit has been developed to define the ROOT data-structures and to provide common functions that can be used across a variety of field data analyses. Tier-1 processing and the production of the non-*art* ROOT files will utilise FermiGrid while algorithm development and the analysis of the non-*art* ROOT files will proceed on local clients e.g. gm2field-server. The data storage and CPU requirements are a small fraction of that required for the ω_a dataset (should quantify this a little better : the context is above ie 25 TB).

VIII. THE MUON $g-2$ COLLABORATION

The Muon $g-2$ Collaboration has nearly 200 members from 35 institutions and 7 countries. Owing to the unique demands of the $g-2$ experiment, and the nature of high-precision physics, the collaboration has been assembled from physics groups that nominally associate themselves with the High-Energy, Nuclear, Atomic, and Accelerator physics communities. To be successful, we have must have experts in all of these areas. We are also supported by a broad external theory community that aims to establish the Standard Model expectation for the muon anomalous magnetic moment.

A. Organization and Governance

The Collaboration organization is illustrated in the following three charts. Figure 6 provides the top-level view of management and the equal Run Coordination and Analysis Coordination arms that reflect the concurrent activities. With the anniversary of assigned positions occurring commensurate with the beginning of the fiscal year (and typical accelerator restart), the names listed represent the second full evolution of this Chart. During the summer shutdown, a transition

process takes place where new leaders begin to work with exiting leaders and start to assume daily responsibilities in time for the new running period.

Figure 7 gives a more detailed breakdown of the responsible individuals for the FY2018 running period. The two Run Coordinators lead the run, schedule the tasks, and chair daily and weekly meetings.

Figure 8 gives the current expected distribution of analysis efforts going forward in the FY18 period. Initial activities have begun based on our FY17 commissioning period. We aim to have a central distribution of the main unpacking and production of raw data at Fermilab, but then enable independent threads or analysis tasks by various teams to extract the precession frequency, the average magnetic field, the key beam dynamics evaluations, and the two required corrections. The two ω_a Analysis Coordinators are at present leading weekly Big Analysis Meeting (BAM) sessions that are open to all collaborators. The ω_p Field Analysis group is beginning to establish their work flow now that first magnetic field data is coming in following the completion of shimming. The Beam Dynamics teams have been meeting weekly for more than a year and they will continue. The Offline Simulation effort is providing realistic pseudo data to test algorithms and to model the beam behavior based on the " as realized" parameters tested to date in the commissioning run. The overall coordination of this very large number of tasks remains open at this point, being steered in the interim by the Co-Spokespersons until the job becomes more defined and demanding. This system is working now quite well.

The governance of the collaboration is described by a series of documents that include the overall Bylaws, the Publication Policy, and the Speakers Policy. Three key committees help steer collaboration business.

- **Institutional Board (IB).** The IB is chaired by a member of the collaboration appointed by the Spokespersons for a 2-year term. Each institution in the collaboration provides a member to the IB; some small institutions are combined with one agreed on representative. The IB Chair runs a business meeting at every collaboration meeting and can call special meetings as needed. The IB Chair organizes the yearly elections of the Co-Spokespersons. The IB decides on collaboration membership, recommends appointments, and generally provides the voice for collaborating institutes.

- **Talks Committee.** The Talks Committee is chaired by a member of the collaboration appointed by the Spokespersons for a 2-year term. Additional members are chosen to represent the breadth of physics, location, and age. The Talks Committee has developed a

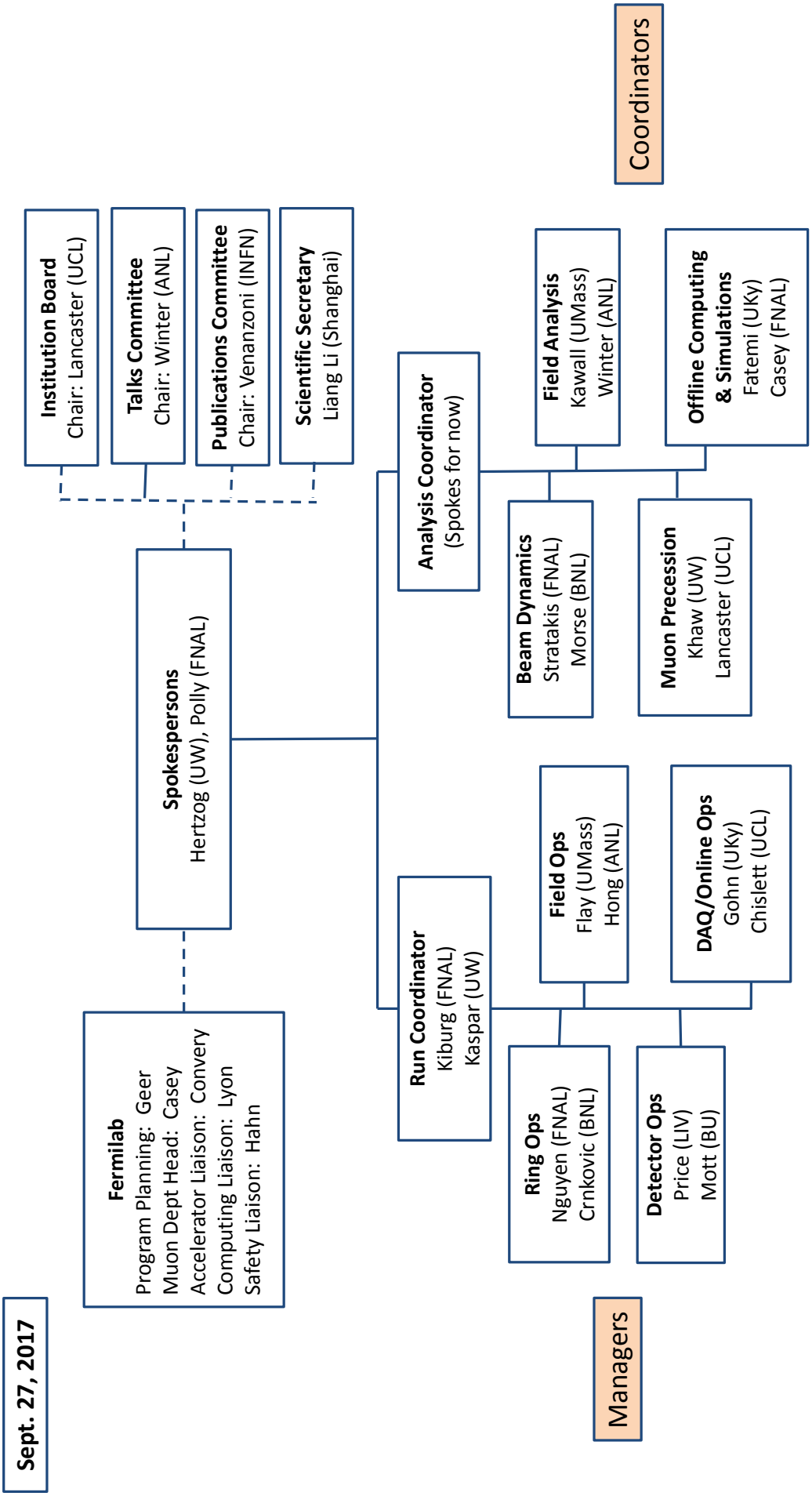

Figure 6: Collaboration Main Organizational Chart – Sept. 2017

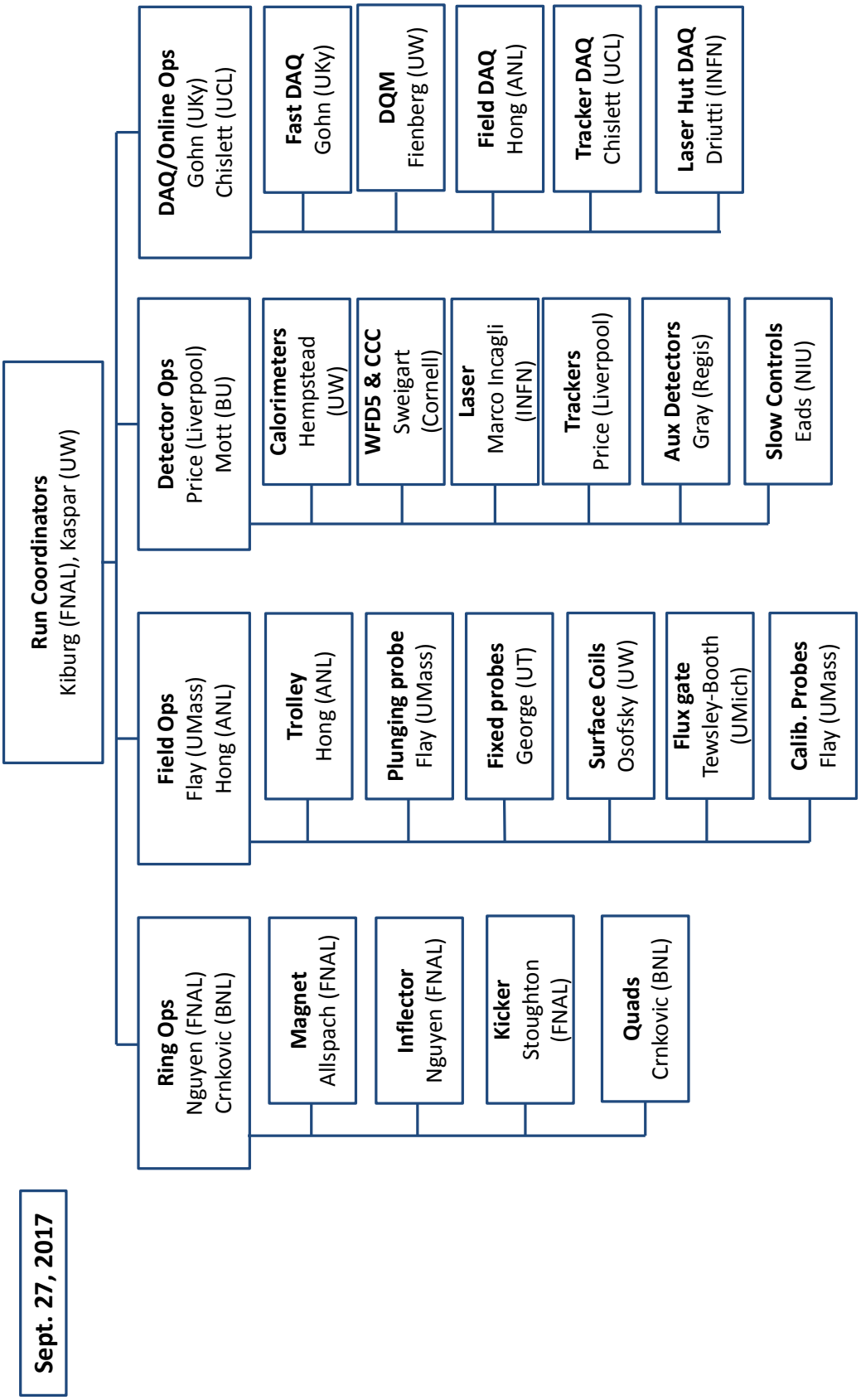

Figure 7: Collaboration Run Coordination Assignments – Sept 2017

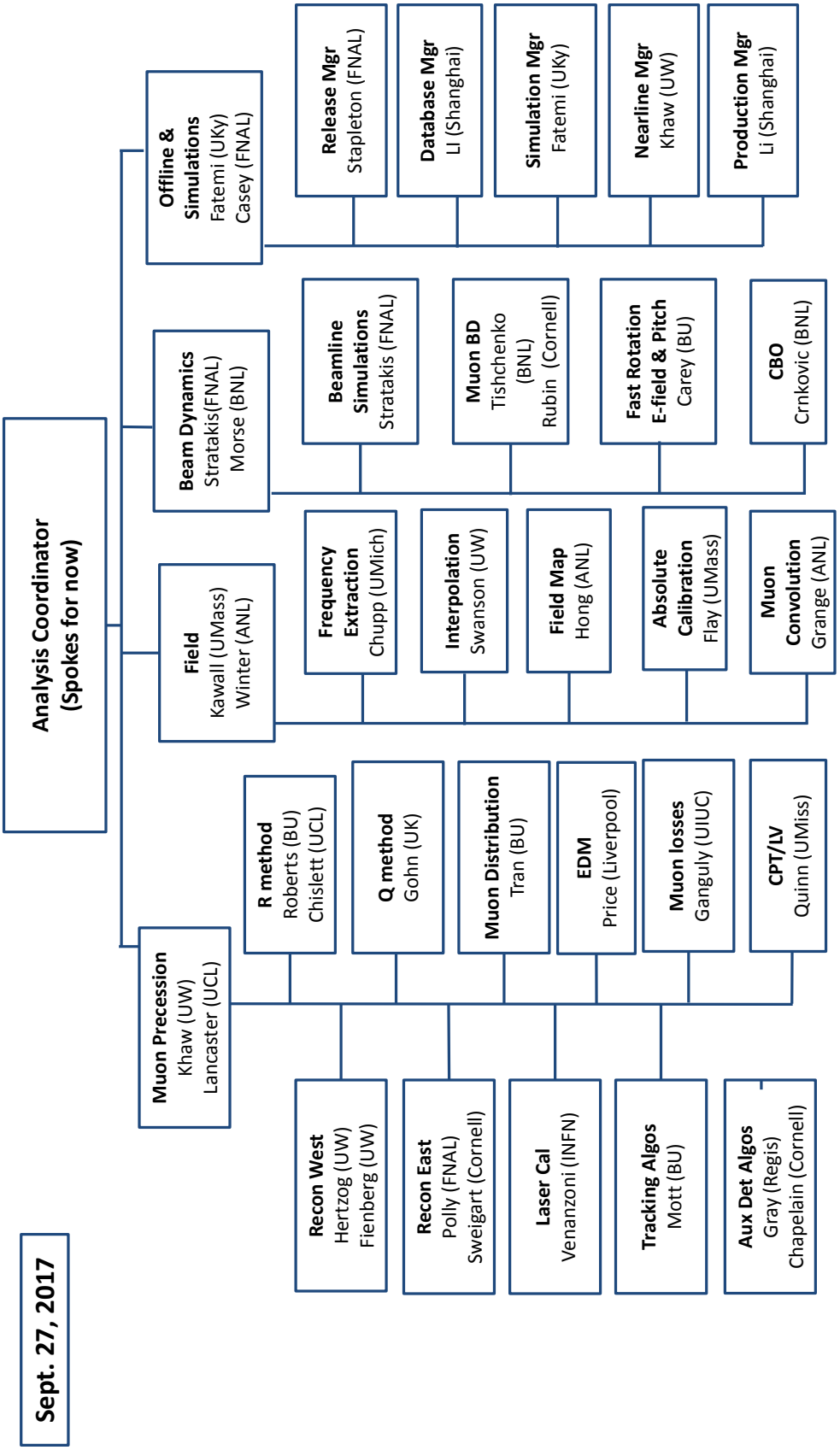

Figure 8: Collaboration Analysis Organization – Sept. 2017

written policy on presentations. The committee distributes talks to deserving members and maintains a data base of efforts.

- **Publications Committee.** The Publications Committee is chaired by a member of the collaboration appointed by the Spokespersons for a 2-year term. Additional members are chosen to represent the breadth of physics, location, and age. The Publications Committee reviews all drafts to be submitted to conference proceedings or to referred journals.

- Scientific Secretary. Liang Li (Shanghai) is the Scientific Secretary for E989. He maintains a detailed database of all collaborators, past and present. He can produce appropriate collaboration lists for publications, reports, and reviews.

B. Shifts

24/7 shift-taking on E989 was in place during the May/June 2017 commissioning run. During that run, shifters were not only assigned to the DAQ and data taking activities, but additional groups assigned shifters to critical hardware, specifically 24/7 monitoring of the Quadrupole system and the Kicker system. Additional collaborators were in the control room nearly at all times to help guide the measuring program.

The E989 shift plan restarts 24/7 operation October 16, 2017 with two weeks of DAQ shifts, which feature exercising the detector systems using our laser system to create pseudo-data sets. Beam commissioning is expected to begin approximately Oct. 30th. c

Shift-taking is expected to be shared equally by E989 collaborators, with the exception of known engineers. A tool has been built for shift signup and shift-point credits. Each collaborator and each institute has a targeted number of shift points to try to obtain. This tool has been introduced to staff the first half of the FY18 run; essentially all shifts are already filled.

Shifter responsibilities include executing the run plan set by the Run Coordinator, verifying that the detectors are running properly, and ensuring that the data is of high quality, as determined from the diagnostic online monitoring. In addition to regular shifters, on-call experts are assigned to provide assistance when problems arise that are beyond the expertise of the shifters. These experts are expected to be contactable 24/7 when they are on call to respond to major issues that are first identified by shifters.

C. Collaboration Institutional Responsibilities

The following list represents a snapshot of the FY18 responsibilities of the Muon $g-2$ institutions as of September, 2017. In each case, a total FTE count follows the institutions name. Specific responsibilities of the institution are identified as a group. An FTE unit is defined as the fraction of *research time*; thus, a faculty member or laboratory scientist spending 100% of her/his time on $g-2$ is counted as 1 FTE in this exercise. Graduate students are counted as 1 FTE regardless of their possible academic course obligations. The commitments are taken from the March, 2017 PI Briefing projected to FY18. Engineers are not counted. Undergraduates are not counted, although there have been many with most groups hosting 1 or more at all times, and expanding considerably in the summer months. We estimate a total of approximately 96 FTEs contributing to the $g-2$ by this accounting scheme. We note that the list below does *not* include the enormous effort by some institutes to design and fabricate various hardware components, nor extensive efforts by many groups to calibrate and install equipment.

National Laboratories

- **Argonne National Laboratory**; FTEs: 3.0; Responsibilities: Collimators, NMR Trolley, Field DAQ, $\omega_p$analysis, Test site for NMR calibrations
- **Brookhaven National Laboratory;** FTEs: 3.0; Responsibilities: Beam dynamics, Beamline simulations, Quadrupole system, CBO analysis
- **Fermi National Accelerator Laboratory;** FTEs: 9.2; Responsibilities: Host institution, Inflector, Storage ring magnet, Surface coils, Vacuum chambers, Kicker operations, Tracker gas, Tracker analysis, Computing support

U.S. University Groups

- **Boston University;** FTEs: 4.1; Responsibilities: Tracker electronics, Tracker analysis, $\omega_a$ratio analysis; Beam dynamics, Machining
- **Cornell University;** FTEs: 5.8; Responsibilities: Blumlein kicker development, Beam dynamics, Storage ring modeling, Waveform digitizers, Clock and controls, $\omega_a$analysis, Fiber harp hardware support and analysis
- **University of Illinois at Urbana-Champaign;** FTEs: 1.85; Responsibilities: Muon loss analysis, $\omega_a$analysis

- **James Madison University;** FTEs: 0.25; Responsibilities: Power management system
- **University of Kentucky;** FTEs: 4.5; Responsibilities: Fast DAQ, Simulations, ω_aQ-method
- **University of Massachusetts;** FTEs: 2.5; Responsibilities: Absolute water probe; Plunging probes, $\omega_p$analysis
- **University of Michigan;** FTEs: 2.67; Responsibilities: Absolute He-3 probe, External magnetic fields
- **Michigan State University;** FTEs: 3.6; Responsibilities: Beam dynamics, COSY beamline model
- **University of Mississippi;** FTEs: 1.5; Responsibilities: Fast rotation analysis, Quadrupole assistance, Lorentz violation analysis
- **North Central College;** FTEs: 0.25; Responsibilities: local university students to help with various tasks
- **Northern Illinois University;** FTEs: 1.5; Responsibilities: Slow control system, Tracker hardware support
- **Regis University;** FTEs: 1.0; Responsibilities: Fiber Harp hardware and analysis, T0 detector
- **University of Texas at Austin;** FTEs: 2.8; Responsibilities: Kicker support software, Fixed probes, $\omega_p$analysis
- **University of Virginia;** FTEs: 0.7; Responsibilities: Muon loss analysis
- **University of Washington;** FTEs: 10.0; Responsibilities: Beam dynamics, Calorimeters hardware, Calorimeter low-level analysis, Data quality monitor, $\omega_a$analysis, NMR probes and multiplexors, Radial field, Surface coil DAQ and modeling, IBMS detectors

International Groups by Country

- **CHINA: Shanghai Jiao Tong University;** FTEs: 2.6; Responsibilities: Database development, Offline production

- **GERMANY: Technische Universitt Dresden;** FTEs: 0.25; Responsibilities: $g-2$ BSM theory
- **ITALY: Laboratori Nazionali di Frascati, INFN: Sezione di Napoli, Sezione di Pisa, Sezione di Roma Tor Vergata, Sezione di Trieste, Universit'à del Molise, Università di Udine;** FTE: 16.2; Responsibilities: Laser calibration system, including laser, optics, monitors, DAQ, flight simulator, analysis, systematic gain studies
- **KOREA: Korea Advanced Institute of Science and Technology (KAIST);** FTEs: 3.0; Responsibilities: RF phase-space damping, Beam dynamics
- **RUSSIA: Novosibirsk Budker Institute of Nuclear Physics and Dubna Joint Institute for Nuclear Research;** FTEs: 3.0; Responsibilities: Paraview event display, Alarm system, MIDAS ODB support (Note: group presently subject to Fermilab site accessibility restrictions)
- **UNITED KINGDOM: Cockcroft Institute, Lancaster University, University of Liverpool, University College London;** FTEs: 13.0; Responsibilities: Tracker hardware, tracker analysis, EDM analysis, tracker DAQ, Beamline modeling, Beam Dynamics, $g-2$ SM theory

IX. FERMILAB ROLES AND RESOURCES

The Muon $g-2$ experiment receives support from the Accelerator Division (AD), Scientific Computing Division (SCD), Technical Division (TD), and Particle Physics Division (PPD).

A. Accelerator Division (AD

AD is responsible for the commissioning, operation, and maintenance of the primary proton beam line, the pion production target, the secondary beamlines M2/M3 and M4/M5, and the Delivery Ring, with its accompanying proton removal kicker. These beamlines must be pulsed at burst rate of 100 Hz, providing 16 injections in to the $g-2$ Storage Ring per 1.4 s machine cycle. AD is responsible for maintenance of all existing standard beamline elements, instrumentation, controls, and power supplies. AD will also be responsible for monitoring intensity and beam quality of the primary proton beam. The quality of beam prepared and delivered to $g-2$ is an integral part of the experimental measurement, and must be understood and maintained in great detail to ensure

a successful experiment. It is important that E989 maintain a close working relationship with AD. That is facilitated by Accelerator Liaison Mary Convery, who is a senior $g-2$ collaborator. It is expected that collaboration members from AD will work closely with non-AD collaborators in preparing and analyzing the injected muon beam.

B. Scientific Computing Division (SCD

SCD is responsible for the supporting the computing needs of the Muon $g-2$ experiment through provision, maintenance, and support of common, and in some cases experiment-specific, core and scientific services and software. These tasks include, but are not limited to, assistance in data storage and retrieval, Monte Carlo and data job submission and production, *art* framework development, and tracking software development. Communication with SCD is done on a frequent basis through Computing Liaison (Adam Lyon), who is also a senior $g-2$ collaborator, and through monthly meetings between the SCD head and the E989 co-spokespersons. Resources are negotiated annually at the SCPMT review.

C. Technical Division (TD)

The TD Cryo Sector is responsible for the operation and maintenance of liquid helium production for the experiment including maintaining the helium tank farm, the A0 compressor building, and the MC-1 cryo plant. TD provides 24/7 on-call support for these systems, conducts weekly walk-throughs of the facilities, and performs regular servicing of compressor and engine components.

D. Particle Physics Division (PPD)

PPD is responsible for the commissioning, operation, and maintenance of the experimental facility beyond the end of the M5 beamline. This includes the cryogenic distribution down stream of liquid helium production, the cryo and storage ring vacuum systems, the inflector and main ring superconducting magnets and power supplies, and all associated controls and monitoring. PPD provides 24/7/365 coverage of one operation shifter in the MC-1 control room for continuous, on-site monitoring. Scientists in the PPD Muon Department collaborate on the commissioning, operation, and maintenance of the electrostatic quadrupoles, the in-ring kickers, and the straw tracker detectors. PPD provides engineering and technical support to the entire experiment.

E. The ESH&Q Department (ESH&Q)

Environment, Safety, Health & Quality is responsible for providing guidance in all ESH&Q matters. The Safety Liaison for Muon $g-2$ is Dee Hahn. Among other responsibilities, she assists collaborators in obtaining required safety training courses at Fermilab.

All safety hazards in MC-1 and mitigations are outlined in the MC-1 Safety Assessment Document [9]. The Muon $g-2$ collaboration promotes a culture where all collaboration members are responsible for safety. Anyone working in MC-1 has the responsibility to report unsafe behavior to their supervisor, the run coordinator, or the ESH&Q liaison. Anyone working in MC-1 has the authority to issue a stop-work for any work being performed unsafely in MC-1.

Access to the MC-1 building is restricted by keyed ID entry to collaborators that have active MC-1 training. All shifters are required to have radiation and controlled access training. A Fermilab employee, the operations shifter, with ODH training is stationed in MC-1 24/7/365 to monitor all equipment and perform any access to ODH areas.

Access to the class 3B laser is restricted to collaborators with laser training. A list of authorized collaborators is maintained by the PPD Saftey Officer and updates require signature approval from the PPD Safety Officer and the PPD Muon Department Head. The laser key is controlled by the operations shifter and is only given to people on the list of authorized collaborators.

Work in MC-1 is performed using the Job Hazard Awareness procedure (JHA). All workers must read, understand, and sign the appropriate JHAs. The Run Coordinator holds a toolbox meeting on days when work is being performed in MC-1 to ensure everyone working in the hall is aware of all hazards. The experiments ESH&Q liaison is present at the toolbox meeting. On days where there was not a toolbox meeting and short jobs are being performed, the work must be approved by the Run Coordinator who is responsible for updating the work crew on any hazards not covered in the JHA.

The experiments ESH&Q liaison will conduct regular walk throughs of the MC-1 building. Any safety issues will be brought to the attention of the run coordinator and discussed at the next toolbox meeting. The PPD Division Office will also conduct monthly walk throughs of the MC-1 building.

X. BUDGET AND RESOURCES

The Operating and Computing Budgets are provided below.

Operating and maintaining the Muon $g-2$ experiment are \$560k in FY18 and \$320k in FY19 and in FY20.

The FY18 computing budget is given per our SCPMT requests. Note that there is an additional tape cost for "migration" because earlier this year Oracle suddenly dropped their tape business and we need to migrate to a different tape technology later in FY18.

Table IV: Detector Operations Budget

Item	FY18 (k$)	FY19 and FY20 (k$)	Notes
Consumables	200	200	Dominated by liquid nitrogen and subject to market fluctuations
Cryo plant upgrades/maintanance	100	20	FY18 based on needed upgrades determined from FY17 operations
Spares	100	10	Spare pool needs to be increased based on known rate of consumption determined in FY17
MC1 power distribution upgrades	70	0	New panel and 30A circuits need to be added
General detector maintenance	60	60	Based on FY17 experience
MC1 building maintenance	30	30	Based on FY15-FY17 experience
Total per year	560	320	

Table V: Computing Operations Budget

Tape	\$ per TB	**SCPMT FY18 Requests**	**Amount**	**Units**	**Cost k$**
T10K Media	30	Data Processing CPU (onsite)	18	M core-hours	180
Migration	30	Simulation CPU (offsite)	9	M core-hours	0
Total tape	60	dCache Tape Backed	400	TB	50
		dCache Scratch	300	TB	38
CPU	\$ per hour	dCache Persistent	200	TB	25
1 Core	0.01	dCache Write Pool	100	TB	13
		NAS Storage	60	TB	9
Disk	\$ per TB	Tape DAQ (2 copies)	4400	TB	264
dCache	125	Tape Reco	1800	TB	108
NAS	150	Tape Simulation	1000	TB	60
		Total Computing and Media			**747**
SCD People	k\$ per FTE				
Support	150	SCD Support Services	10	FTE	1,500

XI. FY18 RUN PLAN AND DETECTOR OPERATIONS

The FY18 run period will expand upon the commissioning run from June 2017. Basic beam systems were commissioned, however the full commissioning plan at the experimental design rate will occur from Nov. 2017 through Jan. 2018. From Feb. 2018 through the end of the run, we anticipate collecting 3 – 5 times the total BNL statistics, where the lower limit is based on measurements achieved during 2017 running.

The run plan for FY18 is designed to optimize detector performance prior to the realization of full beam delivery rate from AD, at which point we anticipate commencing steady state operations.

A. Safety

The key to successful operations will be the safe and stable performance of the shifters and detection systems. Shifters are required to complete FNAL training courses prior to working in the MC-1 hall. Additional radiation safety courses are required for controlled access into the hall. We have developed a close working relationship with PPD Safety Officer Raymond Lewis and solicit his advice during the planning stages for upcoming work.

A shift signup was developed leveraging the experiences of previous collaborations. It was distributed to all eligible collaborators and we have filled shifts through February 2018 with specific collaborator names. On January 8 2018, we anticipate releasing the shift signup for the period of March 2018 through July 2018.

We have established a two-person rule for shifters during the initial run period, and the shifters will be located in the control room at MC-1. At a future date under stable conditions, we will re-evaluate the need for two shifters, and the relocation of the shift location to the ROC-West as appropriate.

In addition, training documents for individual subsystems have been prepared and we have executed several workshops to train individual shifters. These documents are maintained and updated by the system experts to reflect the current conditions. We have also implemented staggered shift blocks, such that every shifter is paired with somebody that was on shift the previous day.

During the shift, it is critical to identify the safe operation and performance of the experimental systems. At the beginning and end of each shift, shifters must complete a checklist developed system experts that documents the status of each of the critical systems. Additionally throughout the shift, periodic checks of data quality parameters are routinely performed. Issues and bugs

with the safe operation of our systems or suggestions for improvements are tracked buy the Run Coordinators via the use of the gm2-runco@fnal.gov listserv.

B. Run plan Nov. 2017 - Jan. 2018

We have based the 2018 run plan on the experience of the 2017 commissioning run. At that time, we observed the regular need to re-establish the timing of our pulsed systems with respect to the delivery of the incoming muon beam. As we were able to train the kicker and quad systems, we also revisited the storage rate as a function of the voltage settings. We anticipate that these sets of scans will be a regular part of the first few months of data collection as the intensity and purity of the muon beam improves. Additionally, we will be integrating the rest of the systems that operated somewhat independently during the commissioning run, in order to achieve a holistic approach towards data collection.

We have worked closely with AD to develop an understanding of the anticipated arc for the improvement of the muon beam. With the goal of reaching stable operating conditions during January, we have the following key dates in mind:

Oct 16: 24/7 Shift coverage begins:

- All systems operating, being monitored by shifters.
- Laser calibration of the calorimeter energy scale prior to arrival of beam
- Reinstallation of trolley, plunging probe in vacuum

Oct 30: Shutdown ends; AD begins beam preparation, but no beam to $g-2$

- Laser calibration of the calorimeter energy scale prior to arrival of beam
- Final reinstallation of in-vacuum equipment
- Establish storage ring vacuum
- Establish full field measurement (calibrated trolley + plunging probe in storage ring)
- Interlock hall by end of week

Oct 30: Commence establishing beam in M5 line

- Integration of the upgraded Incoming Beam Monitoring System (IBMS) into the data acquisition system.

- Integration of our beam monitoring tools in parallel with the accelerator division beam delivery tools.
- Investigation and understanding of the injection handoff at the storage ring interface
- Establish beam to ring

Nov 7 - Nov 28: AD works on Delivery Ring orbits and proton removal

- Laser calibration prior to beam
- Establish periodic trolley runs to evaluate stability and continue to refine field shape via surface coil current distributions
- Establish storage rates as a function of injection parameters (Quad high voltage, quad scraping studies, Kicker HV, Kicker timing, Inflector current, M5 line magnet settings in conjunction with Main magnet current). Note, this are generally independent scans where the other parameters in the scan are set to their previously developed optimums. We will then push to understand couplings in the optimums
- Establish beam measurement of the average radial field utilizing surface coils to nullify vertical offset in the beam distribution
- Perform periodic full field scans and establish stability
- Upgrade of Storage Ring Vacuum pumping system that permits design performance of the in-vacuum pulses systems. Scheduled to occur mid November and will be scheduled to install opportunistically during the early morning shift prior to daily Delivery Ring work (day+owl shift)

December 2017: AD beam to experiment while increasing rep rate and efficiency

- Regular repeats of scans of storage rate as a function of injection parameters
- Regular (each shift) kicker timing scans to verify understanding of the detector and its status
- Establish beam profile and CBO amplitude via the tracker system
- Establish storage sensitivity to beam steering and quantifying beam losses via to the collimator systems

- Laser calibration of the calorimeter energy scale interleaved with beam
- Regular (weekly) fiber harp calibrations as the beam delivery rate increases.
- Full anlysis chain recommissioning at nominal rate

January 2018: AD tunes up beam - approaching production

- Cross calibration of beam dynamics parameters utilizing trackers and fiber harps
- Periodic rescans of key injection parameters to characterize stability
- Regular (weekly) fiber harp calibrations as the beam delivery rare increases
- Regular (3 times per week) field measurements
- Full detector operation
- Full pulsed system operation
- Demonstrate long-term stability of all systems and reproducibility of their performance parameters prior to establishing the steady state beam delivery.(Perform week-long stability studies at proposed operating conditions)

C. Run plan Feb. 2018 - Jul. 2018

During this period we anticipate running with steady-state operations at a storage rate that should accumulate (3 – 5) times achieved at Brookhaven. This estimate is obtained by careful examination of all of the systems that operated successfully during the 2017 running and modifying the observed rates with planned updates.

During this period we will operate in a mode that focuses on stable run conditions of our magnets, as well as the pre-planned operating voltages of the kicker and quadrupole systems. We will also deploy field measurements that optimizes the statistical and systematic contributions to the result, while minimizing systematic biases from environmental factors by performing the measurements on an irregular pseudorandom schedule.

---

[1] A. Czarnecki and W. J. Marciano, Phys.Rev. **D64**, 013014 (2001).

[2] M. Davier, in *14th International Workshop on Tau Lepton Physics (TAU 2016) Beijing, China, September 19-23, 2016* (2016), 1612.02743, URL http://inspirehep.net/record/1502365/files/arXiv:1612.02743.pdf.

[3] G. Bennett et al. (Muon g-2 Collaboration), Phys.Rev.Lett. **92**, 161802 (2004).

[4] L. Jin, T. Blum, N. Christ, M. Hayakawa, T. Izubuchi, C. Jung, and C. Lehner, in *Proceedings, 34th International Symposium on Lattice Field Theory (Lattice 2016): Southampton, UK, July 24-30, 2016* (2016), 1611.08685, URL http://inspirehep.net/record/1500525/files/arXiv:1611.08685.pdf.

[5] V. Bargmann, L. Michel, and V. Telegdi, Phys.Rev.Lett. **2**, 435 (1959).

[6] G. Bennett et al. (Muon G-2 Collaboration), Phys.Rev. **D73**, 072003 (2006).

[7] D. Hanneke, S. Fogwell, and G. Gabrielse, Phys. Rev. Lett. **100**, 120801 (2008), 0801.1134.

[8] C. Group, *CODATA 2014 Recommended Values (online).* (2014).

[9] See: https://gm2-docdb.fnal.gov/m document #5095 for Excerpts of the Fermilab SAD for Muon Campus and g-2

Acronyms

ACNET	Accelerator Control Network
AD	Accelerator Division
BSM	Beyond the Standard Model
CY	Calendar Year
DAQ	Data Acquisition System
DocDB	Document Database
ESH&Q	Environment, Safety, Health and Quality
FY	Fiscal Year
GPS	Global Positioning System
GPU	Graphical Processing Unit
IB	Institutional Board
M&S	Materials and Supplies
NMR	Nuclear Magnetic Resonance
OSG	Operation Support Group
POT	Protons on Target
PS	Power Supply
PP	Plunging NMR Probe
SCD	Scientific Computing Division
SM	Standard Model of Particle Physics

Appendix A: SPARES

Each area has been asked to survey their list of spares. Of course there are critical one-only items, such as the Storage Ring, but here we provide lists and comments about the supportive instrumentation and magnets.

The AD is a reliable partner with a comprehensive track record of maintaining systems of spares for the different types of magnets used in the system. They have at least one spare of each type of magnet, DC power supply, and instrumentation device in the beamlines used for $g-2$. For the pulsed power supplies built at Fermilab, spare parts are on hand. Spares do not exist for some specialty beampipe components such as expensive bellows or the "pants leg" section of pipe where the M2 line merges into the M3 line. The expected lifetime of the target station components is longer than the lifetime of the $g-2$ experiment. A spare target of an old Pbar design, 3 spare lithium lens assemblies — though they are externally cooled rather than internally cooled — and 2 spare pulsed momentum-selection magnets all exist.

The following tables are provided by various subsystem groups.

Table VI: Calorimeters and Digitizers

Item	No. Employed	Spares	Comment
Calibration lasers	6	1	Only 3 are needed for running
Calorimeter crystals & SiPMs	1296	25	No failures once running
Low voltage power supplies	24	2	Can replace and repair in < 4h
WFD5 5 channel digitizers	312	8	Includes 1 hot spare in 23 of the 24 calorimeter stations
FC7-R2 (CCC)	6	1	
EDA-02707 FMC (CCC)	9	3	
EDA-02708 FMC (CCC)	5	7	
HiTech Global HTG-FMC-SMA-LVDS	1	2	2 in October purchase
Vadatech MCH	31	4	
AMC13	31	7	
Vadatech Power module	31	4	
uTCA crate (Al)	24	2	
uTCA (retro Al)	5	0	
uTCA (steel)	2	0	
Avago AFBR-703SDZ 10 Gbit SFP+	31	2	
Finisar FTLF1318P3BTL SFP (TTC)	81	2	
CU Clock multiplexer boards	27	3	30 in production
Beaglebone blacks	27	3	30 in October purchase
SRS FS725/1C 10 MHz Rb Freq Stdrd	3	1	2 in October purchase
SRS SG382 10 MHz Freq Synthesizer	1	1	
SRS SR620/1 Frequency Counter	2	1	2 in October purchase
SRS FS740 GPS-disc. 10 MHz Stdrd	1	1	2 in October purchase; spare provides backup for both a 10 MHz source or the meridian receiver.
Meridian GPS receiver	1	0	
Wenzel LNFD-4-40-13-1-13	1	1	
Minicircuits ZP-1MH+	1	2	

Table VII: Straw Trackers

Item	No. Employed	Spares
Straw Tracker Modules	16	6
FC7 readout cards	2	3
Logic Boards	32	30
TDC Boards	128	27
ASDQ Boards	128	160
SFPs	32	18
HV Boards	32	37
LV Boards	16	10
LV AC/DC Crates	2	1
HV Crates	4	2
HV Modules	32	8
Readout/Control PCs	3	1

Table VIII: Laser Calibration System

Item	No. Employed	Spares
Laser Heads	6	3
Laser drivers	6	1
Multichannel driver SepiaII	1	0
Filter wheels	6	1
Source monitor (int sphere)	6	1
Mini-bundles optical fibers	6	1
Mini-pc	1	1
HV crates	1	1
HV modules	7	7
Preamplifier boards for LM	5	4
LV AC/DC Crate	1	1
PMTs for LM	24	30
Optical components (mirros, cubes splitting, collimators)	66	12
Custom electronics crate	1	1
SM boards	6	1
Preamplifier boards for SM	6	1
Launching optical fibers 25 m long	24	3
Monitor optical fibers 25 m long	24	36
Light distribution boxes (fiber bundle, diffuser, light distr plate)	24	2
Motorized Flipper Optical Mounts for double pulse test	6	0
Digital delay generator for double pulse test	1	0
Mirrors for double pulse test	18	2

Table IX: Magnetic Field Measurement Systems

Item	No. Employed	Spares	Comment
Fixed NMR Probes	378	2	some parts at CENPA, cannot be replaced unless vacuum chambers removed
Trolley NMR Probes	17	17	–
Trolley Mulitplexer	1	0	one untested spare at ANL
Trolley NMR analog electronics	1	0	–
Trolley NMR controller	1	1	–
Trolley interface	1	1	–
FP NMR Multiplexers	20	2	can replace if needed easily
FP NMR pulser-mixers	20	2	can replace if needed easily
FP multiplexer power	1	0	parts at CENPA for another
FP VME 64X crate	1	0	–
FP Acromag carrier board	1	1	–
FP Acromag DIO daughter boards	3	2	can obtain from ANL
FP FPGA daughter boards	1	1	–
FP VME Controller	1	0	can obtain 1 spare from ANL
FP Digitizers	2	0	can obtain 1 spare from PP
Frequency Generators	3	0	can obtain 1 spare short-term from ANL
Distribution Amplifiers 62 MHz	2	1	–
Distribution Amplifiers 10 MHz	1	1	–
Rubidium Clock	1	1	–
Frequency Counter	1	0	–
PP commercial electronics	1	0	spares for most parts at ANL
PP custom electronics	1	0	spares under construction